Dynamic Behaviour of Pile Foundations in Layered Soil Half-Space Using Cone Method

M.M. Aldimashki[1] and J.M.W. Brownjohn[2]

[1,2] *Department of Civil and Structural Engineering, University of Sheffield, Sir Frederick Mappin Building, Mappin Street, Sheffield, S1 3JD, UK. 0114 222 5771*

[1] *corresponding author*

James.brownjohn@sheffield.ac.uk

+44 0114 222 5771

Abstract

The dynamic behaviour of pile foundations embedded in a horizontally stratified soil profile is investigated using the Cone method, which applies only for shallow foundations. In this paper dynamic impedance functions have been generated for several cases using an enhanced cone frustum approach which deals with the drawback of negative damping in the current approach. The frequency domain approach can be implemented in systems modelled using the spectral elements. Comparison with the coupled Finite Element-Boundary Element (FE-BE) method shows a good correlation with the proposed method which does not use transformation to the wave-number domain.

Introduction

In industrial facilities which consist of a number of sensitive machines, if any item of equipment malfunctions due to excessive vibration or settlement of the foundations, a substantial effect on the overall performance of the facility could be catastrophic [Chowdhury & Dasgupta, 2009]. Therefore if proper attention is not paid to the design of foundations, consequences could be quite far reaching and serious in nature.

The strength-of-materials approach using cones [Wolf, 1994] to model foundations embedded in infinite soil media leads to physical insight with conceptual clarity. The treatment of foundations embedded in half-space using Cone models has been initialised by Meek & Wolf [1994] and has been performed using a stack of embedded disks covering the volume of the foundation. The development of the Cone models for layered media in foundation vibration engineering has encountered different phases but two main types of approach exist in all these phases.

The first type is characterised by the concept of one-dimensional wave propagation in cone segments with reflections and refractions occurring at material interfaces in multiple-layered half-space where it is possible to track the reflection and refraction of each incident wave sequentially and determine the resulting wave pattern up to a certain stage by superposition [Wolf & Preisig, 2003]. There are limitations to this type of approach, particularly related to the depth of the disk embedded in the soil profile. It is argued [Wolf & Deeks, 2004a] that for an embedment that is an order of magnitude larger than the radius of the disk such as a pile foundation, modifications of the flexibilities have to be performed to use Cone models.

The second type of analysis is introduced by Wolf & Meek [1994b] to study the vibrations of a foundation on the surface of or embedded in a layered half-space, based on the so-called backbone cone which is generated by specifying the cone frustums

through which the wave propagation takes place. The layered half-space is divided into slices where rigid disks are confining segments of cone frustums at top and bottom while free boundaries are assigned to the remaining parts of the slices beyond the cone frustums with reflections only occurring within these free boundaries. After assemblage, the dynamic-stiffness matrix of the multiple-layered half-space is obtained, which can be used to calculate the dynamic-stiffness matrix of the foundation. Although this procedure (called cone frustums) is generally applicable, there is a possibility that the radiation damping can become negative, which is physically impossible. A similar approach, based on a modified cone frustum method, is outlined by Jaya & Prasad [2002] to study the dynamic behaviour of foundations embedded in a layered half-space in which the boundaries of soil slices beyond the cone frustums are not assumed free and the reflections within the slices depend on the soil properties of each slice and the two slices overlying and underlying it using an effective reflection coefficient. The same concept is extended for pile foundations later [Jaya & Prasad, 2004]. However this modified model is mainly based on the work of Meek [1995] which handles a foundation embedded in a dynamic system consisting of a layer with half-spaces on top and bottom. This case is not relevant to the general layered profiles comprising multiple soil layers overlying each other. Also the results of this modified model for pile foundations have not been compared to the original one of Wolf & Meek [1994b] in layered profiles. Furthermore the problem of negative damping in the dynamic stiffness matrices of cone frustums has not been addressed in the modified model.

An enhanced model based on the cone frustum approach of Wolf & Meek [1994b] is presented in this paper and is compared to the original cone frustum approach, the conventional Novak's method and also to the coupled Finite Element-Boundary Element method. The main drawback of cone frustum approaches, yielding negative damping, is treated by setting the negative values of damping to zero. Among the

current available Cone methods for modelling pile foundations in layered profiles, the proposed enhanced model is less demanding than other ones in terms of computational cost since no tracking of wave propagation is required and no reflection coefficients are calculated to carry out the analysis. The following section gives an overview of the Cone model used in the enhanced model. It is worth mentioning that only compressible soil with Poisson's ratio less than 1/3 is addressed in this paper.

Overview of Cone Model

Linear behaviour of the site is assumed, hence the soil is assumed to remain linearly elastic with hysteretic material damping during dynamic excitation. Figure 1 shows the soil below a loaded disk, modelled as a truncated rod (bar) with its area varying as in a cone which is called an initial cone with outward wave propagation [Wolf, 1998]. The height of the cone's apex is denoted z_0 and z_0 / r_0 is defined as the aspect ratio. This ratio, which defines the opening angle of the cone, only depends on the Poisson's ratio ν of the soil layer through which the resulting wave travels, and the degree of freedom considered. Table 1 [Wolf, 1994] gives the values of aspect ratios for different types of motion in terms of the Poisson's ratio ν, dilatational wave velocity c_p and shear wave velocity c_s.

To model an embedded foundation, the interior soil region is viewed as a stack of rigid disks separated by soil layers as shown in Figure 2 where a pile foundation embedded in a layered half-space is modelled by the corresponding disks at interfaces. This will lead to the dynamic stiffness of the pile foundation as will be demonstrated later.

In order to obtain good accuracy in all cone approaches, the soil region should be discretised in such a way that the thickness of any soil slice should not exceed one tenth of the shortest wavelength λ of the propagating waves. The maximum vertical distance

Δe between two neighbouring disks, as shown in Figure 2, should satisfy the rule: [Wolf & Deeks, 2004a]

$$\Delta e \le \frac{\lambda}{10} = \frac{\pi c}{5\omega_{\max}} \tag{1.1}$$

where $\omega_{\max}$ represents the highest frequency the dynamic model will experience and c is the relevant wave velocity (dilatational for vertical and rocking motions or shear for horizontal and torsional motions).

The vertical degree of freedom of a disk overlying or embedded in a layered half-space will be addressed for the following demonstration. All other degrees of freedom including horizontal, rocking and torsional can be handled analogously. The concept consists of first specifying the so-called backbone cone of the profile, which determines the radii of the disks at the upper and lower interfaces of each cone frustum as shown in Figure 3. Discretization of the soil layers into the necessary number of slices will follow to define the final geometry of the backbone cone. The dynamic stiffness matrices of all the cone frustum segments are then calculated and subsequently assembled together with the underlying half-space to form the dynamic stiffness matrix of the corresponding backbone cone. Applying a unit load at the disk and solving for the displacement amplitudes at all disks leads to a column in the flexibility matrix $[G^f(\omega)]$ of the free field (or virgin half-space). This procedure is repeated for all disks and their corresponding backbone cones as illustrated in Figure 4 to obtain all columns of $[G^f(\omega)]$. The following sections provide the necessary equations of the method under the translational and rotational motions.

Translational motion

The dynamic stiffness of a single cone modelling an incident wave induced by a disk load of radius r_1 on a half-space is given by: [Wolf & Meek, 1994b]

$$S_1(\omega) = K_1\left(1 + i\,\frac{\omega z_0}{c}\right), \tag{1.2}$$

$$K_1 = \frac{\rho c^2 \pi r_1^2}{z_0} \tag{1.3}$$

where K_1 is the static translational stiffness coefficient of the cone modelling the incident wave, c is the relevant wave velocity, ω is the load circular frequency and ρ is the soil density.

Also the dynamic stiffness of a single cone modelling the reflected wave of the same disk load at a disk of radius r_2 at the lower interface of the cone frustum segment presented in Figure 4 is given by: [Wolf & Meek, 1994b]

$$S_2(\omega) = K_2\left(1 + i\,\frac{\omega(z_0 + t)}{c}\right), \tag{1.4}$$

$$K_2 = \frac{\rho c^2 \pi r_2^2}{z_0 + t} \tag{1.5}$$

where K_2 is the static translational stiffness coefficient of the cone modelling the reflected wave and t is the thickness of the cone frustum segment.

The layered half-space is divided into slices where rigid disks are confining segments of cone frustums at top and bottom while free boundaries are assigned to the remaining parts of the slices beyond the cone frustums with reflections only occurring within these free boundaries as observed in Figure 4. The forces acting on the top and bottom disks and their corresponding displacements are related as:

$$\begin{Bmatrix} P_1(\omega) \\ P_2(\omega) \end{Bmatrix} = [S(\omega)] \begin{Bmatrix} u_1(\omega) \\ u_2(\omega) \end{Bmatrix} \tag{1.6}$$

The dynamic stiffness matrix of the cone frustum segment $[S(\omega)]$, which has been shaded in Figure 4, is given by: [Wolf & Meek, 1994b]

$$[S(\omega)] = \frac{S_1(\omega)}{T_{11}(\omega)T_{22}(\omega) - T_{12}(\omega)T_{21}(\omega)} \begin{bmatrix} T_{22}(\omega) & -\frac{S_2(\omega)}{S_1(\omega)}T_{21}(\omega) \\ -T_{12}(\omega) & \frac{S_2(\omega)}{S_1(\omega)}T_{11}(\omega) \end{bmatrix} \tag{1.7}$$

where $T_{11}(\omega), T_{12}(\omega), T_{21}(\omega), T_{22}(\omega)$ are functions representing wave reflections within the soil slice and can be calculated as shown in Appendix 1.

There will be some negative complex values in the dynamic stiffness matrix of each cone frustum segment as reported by some authors [Pradhan et al., 2004; Wolf & Preisig, 2003]. These values will be set to zero in this paper because it is not physically possible to have negative values for the complex parts of the stiffness matrices.

Rotational motion

Similarly to the translational motion, the dynamic stiffness of a soil cone segment modelling an incident wave induced by a moment load acting on a disk of radius r_1 on a half-space is given by: [Wolf & Meek, 1994b]

$$S_{\vartheta 1}(\omega) = K_{\vartheta 1}\left[1 - \frac{1}{3}\frac{(\omega z_0/c)^2}{1+(\omega z_0/c)^2} + i\,\frac{\omega z_0}{3c}\frac{(\omega z_0/c)^2}{1+(\omega z_0/c)^2}\right], \tag{1.8}$$

$$K_{\vartheta 1} = \frac{3\rho c^2 I_0}{z_0} \tag{1.9}$$

Also the dynamic stiffness of a single cone modelling the reflected wave of the same moment load at a disk of radius r_2 at the lower interface of the cone frustum segment is given by: [Wolf & Meek, 1994b]

$$S_{\vartheta 2}(\omega) = K_{\vartheta 2}\left[1 - \frac{1}{3}\frac{\left(\omega(z_0+t)/c\right)^2}{1+\left(\omega(z_0+t)/c\right)^2} + i\,\frac{\omega(z_0+t)}{3c}\frac{\left(\omega(z_0+t)/c\right)^2}{1+\left(\omega(z_0+t)/c\right)^2}\right], \tag{1.10}$$

$$K_{\vartheta 2} = \frac{3\rho c^2 I_0}{z_0+t} \tag{1.11}$$

where $K_{\vartheta 1}$ and $K_{\vartheta 2}$ are the static rotational stiffness coefficients of the cones modelling the incident and reflected waves, $I_0 = \frac{\pi\, r_0^4}{4}$ and $c = c_p$ for rocking motion, $I_0 = \frac{\pi\, r_0^4}{2}$ and $c = c_s$ for torsional motion with $r_0 = r_1$ for $K_{\vartheta 1}$ and $r_0 = r_2$ for $K_{\vartheta 2}$.

The moments acting on the top and bottom disks and their corresponding rotations are related as:

$$\begin{Bmatrix} M_1(\omega) \\ M_2(\omega) \end{Bmatrix} = [S_\vartheta(\omega)] \begin{Bmatrix} \vartheta_1(\omega) \\ \vartheta_2(\omega) \end{Bmatrix} \tag{1.12}$$

The dynamic stiffness matrix of the cone frustum segment $[S_\vartheta(\omega)]$ can be calculated similarly to the translational motion equation and the relevant transfer functions are given in Appendix 1.

Dynamic Stiffness of the Soil-Pile System

The dynamic stiffness matrix $[S^f(\omega)]$ of the free field, which is the inverse of the flexibility matrix $[G^f(\omega)]$, is discretised in the nodes corresponding to the rigid disks. The following approach was proposed by Wolf [1994] for piles embedded in a

homogeneous half-space and it is extended to a layered half-space in this paper based on the previously detailed approach.

Replacing the soil region by the pile material results in a dynamic stiffness matrix $[\Delta S^f(\omega)]$ with the same discretisation but different properties of the pile and soil, which can be calculated using the relevant equation from the following:

$$[\Delta S^f(\omega)] = [\Delta K_{hr}] - \omega^2[\Delta M_h] - \omega^2[\Delta I_r] \text{ for horizontal and rocking motions,} \quad (1.13)$$

$$[\Delta S^f(\omega)] = [\Delta K_v] - \omega^2[\Delta M_v] \text{ for vertical motion,} \quad (1.14)$$

$$[\Delta S^f(\omega)] = [\Delta K_t] - \omega^2[\Delta I_t] \text{ for torsional motion,} \quad (1.15)$$

where:

$[\Delta K_{hr}]$, $[\Delta K_v]$, $[\Delta K_t]$ are the matrices of differences in the static horizontal and rocking, vertical and torsional stiffness properties respectively of pile and soil solid cylinders within the length t.

$[\Delta M_h]$, $[\Delta M_v]$ are the matrices of differences in the mass properties of pile and soil solid cylinders for the horizontal and vertical motions respectively.

$[\Delta I_r]$, $[\Delta I_t]$ are the matrices of differences in the mass moment of inertia and the polar mass moment of inertia respectively of the pile and soil solid cylinders.

All matrices are discretised at the disk positions, similar to $[S^f(\omega)]$ and are given in Appendix 2.

Since the horizontal and rocking motions of a single pile are coupled when handling the lateral motion, both displacements and rotations should be considered in the horizontal direction as shown in Appendix 2, where the first and third columns of $[\Delta K_{hr}]$ correspond to lateral displacements while the second and fourth columns correspond to

rotations. However there is no coupling in the vertical and torsional directions and only vertical displacements and torsional rotations are considered in the matrices $[\Delta K_v]$ and $[\Delta K_t]$ respectively as shown in Appendix 2.

Then the force–displacement relationship of the pile foundation can be established as:

$$P(\omega) = \left([S^f(\omega)] + [\Delta S^f(\omega)]\right) u(\omega) \tag{1.16}$$

where the sum $[S^f(\omega)] + [\Delta S^f(\omega)]$ represents the dynamic stiffness matrix of the pile embedded in soil discretised in all nodes corresponding to the disks. The inverse of this matrix represents the dynamic flexibility matrix $[G(\omega)]$ of the coupled soil-pile system. The reciprocal of the first element in the flexibility matrix is the frequency-dependent dynamic stiffness of the pile's head $S^p(\omega)$ and it takes the form:

$$S^p(\omega) = k^p(\omega) + i\,\omega\, c^p(\omega) \tag{1.17}$$

where the real part $k^p(\omega)$ is the dynamic stiffness coefficient and the imaginary part $c^p(\omega)$ is the damping coefficient.

The soil damping can be considered by using the correspondence principle which defines the complex wave velocities as follows: [Wolf, 1985]

$$c_s^* = c_s\sqrt{1+2i\,\zeta} \tag{1.18}$$

$$c_p^* = c_p\sqrt{1+2i\,\zeta} \tag{1.19}$$

where c_s^*, c_p^* are the complex shear and dilatational wave velocities respectively and ζ is the soil hysteretic damping ratio.

The following section will investigate a numerical example of a pile foundation embedded in different soil profiles using the proposed enhanced method and other ones for comparison.

Numerical Example

A pile foundation that has a radius of 0.3 m and a length of 20 m is embedded in the four different soil profiles shown in Figure 3.5 and denoted P1, P2, P3 and P4. The ratio of modulus of elasticity of the pile to that of the bottom half-space, $E_p / E = 100$, Poisson's ratio $\nu = 0.3$ for all layers, the ratio of mass density of pile to that of the soil layers $\rho_p / \rho = 1.25$ and the soil hysteretic damping ratio $\zeta = 5\%$ for all layers. The results of the enhanced cone frustum method, which will be referred to as 'Enhanced CF model' are compared with the original cone frustum model which in turn will be referred to as 'CF model'. A reference model, obtained from the coupled Finite Element-Boundary Element method, using the Elasto-Dynamics Toolbox (EDT) is also used. EDT is a MATLAB toolbox used to model wave propagation in layered soils based on the Boundary Element method [Schevenels et al., 2008]. It allows to calculate the forced response of the soil due to a disk load (i.e. the flexibility functions), which can be used to calculate the foundation impedance functions [Schevenels et al., 2009]. The same procedure explained before is used to calculate the dynamic stiffness and damping coefficients of the pile foundation using EDT. The solution obtained using EDT will be referred to as 'FE-BE model' since it couples the stiffness of the finite pile elements with the stiffness of the boundary elements of the soil profile.

Another conventional approach to the impedance functions of pile foundations, developed by Novak and his co-workers [Novak & Aboul-Ella, 1978] is also checked and compared with the three analytical methods. This approach is based on the dynamic soil reactions in the relevant degree of freedom [Novak et al., 1978] using viscoelastic materials with hysteretic damping.

Figures 3.6, 3.7, 3.8, 3.9, 3.10 and 3.11 show the horizontal, vertical and rocking stiffness and damping coefficients of the pile foundation embedded in the four soil

profiles using the FE-BE model, CF model, enhanced CF model and Novak's model. The simulations show that the correlation between the enhanced CF model and the FE-BE model, which is considered as the exact solution in Elasto-Dynamics [Wolf & Deeks, 2004a], is very good in all degrees of freedom and is always better than both Novak's model and CF model. However both CF models and Novak's model overestimate the damping coefficient over the low frequency range (<5 Hz) in the translational degrees of freedom. One reason for this phenomenon in CF models is the rigidity of the disks that are flexible in the FE-BE models. Nevertheless the enhanced CF model provides a better agreement in overall values compared with the FE-BE model. The impact of cancelling negative damping in the enhanced CF model can be observed in the stiffness coefficients of the pile foundation embedded in the four soil profiles where the correlation with the FE-BE model becomes better than the original CF model, especially in the layered profiles.

Figure 6 and Figure 7 show that the very top layer determines the value of the horizontal stiffness coefficient regardless of the underlying layers and as a result the piles in profiles P3 and P4 have mostly similar stiffness coefficients. Moreover the horizontal stiffness coefficient changes proportionally with the variation of the stiffness of the top layer. This observation is less evident in the vertical direction as shown in Figure 8 and Figure 9 where all the soil layers contribute to the value of the stiffness coefficient. Consequently the pile in profile P4 is stiffer than the pile in profile P3 in the vertical direction since its lower half is embedded in the full strength half-space. Also the rocking degree of freedom is much influenced by the properties of the top layers as shown in Figure 10 and Figure 11 and hence the piles in profiles P3 and P4 have close stiffness and damping coefficients.

Conclusions

The dynamic behaviour of pile foundations embedded in a horizontally stratified soil profile has been investigated in this paper using an enhanced cone frustum model to evaluate their dynamic impedance functions for different configurations of layered profiles. Compared to the current cone frustum approach, the proposed enhanced approach has treated the main drawback of getting negative radiation damping in the current one.

It has been shown that the dynamic stiffness and damping coefficients obtained from the enhanced cone frustum model of pile foundation embedded in layered profiles correlate very well with the coupled Finite Element-Boundary Element method for all degrees of freedom over the whole considered frequency range. This correlation is better than the current cone frustum model and Novak's model, particularly in the layered profiles. In general the proposed Cone model shows a good agreement with the FE-BE method for pile foundations embedded in layered profiles.

Another advantage of the proposed Cone model is that the transformation to the wave-number domain is not necessary, compared with the analysis in the Boundary Element method. Also no tracking of wave propagation is required to perform the analysis. Therefore it is significantly less demanding than all previous methods in terms of computational cost. Moreover the Cone model provides a clear physical insight of the propagation process and describes the free field motion first and then accounts for any embedded part in the soil medium. This feature makes it possible to study the soil-foundation interaction problem under any source of excitation whether it is acting on the surface of the profile or is propagating from a seismic source. The analysis is limited to small amplitudes of strain since only the linear properties of soil layers were used throughout the proposed procedure.

Appendix 1

Transfer functions in translational motion [Wolf & Meek, 1994b]:

$$T_{11}(\omega) = 1 + 2\sum_{j=1}^{\infty} \frac{e^{-ij\,\omega T}}{1 + j\,2t\,/\,z_0} \tag{1.20}$$

$$T_{21}(\omega) = 2\sum_{j=1}^{\infty} \frac{e^{-i\,(j-0.5)\,\omega T}}{1 + (j-0.5)2t\,/\,z_0} \tag{1.21}$$

$$T_{12}(\omega) = 2\sum_{j=1}^{\infty} \frac{e^{-i\,(j-0.5)\,\omega T}}{1 + (j-0.5)2t\,/\,(z_0 + t)} \tag{1.22}$$

$$T_{22}(\omega) = 1 + 2\sum_{j=1}^{\infty} \frac{e^{-ij\,\omega T}}{1 + j\,2t\,/\,(z_0 + t)} \tag{1.23}$$

Transfer functions in rotational motion [Wolf & Meek, 1994b]:

$$T_{11}(\omega) = 1 + 2\sum_{j=1}^{\infty} e^{-ij\,\omega T} \left[\frac{1}{\left(1 + j\,2t\,/\,z_0\right)^2} + \left\{ \frac{1}{\left(1 + j\,2t\,/\,z_0\right)^3} - \frac{1}{\left(1 + j\,2t\,/\,z_0\right)^2} \right\} \frac{1}{1 + i\,\omega z_0\,/\,c} \right] \tag{1.24}$$

$$T_{21}(\omega) = 2\sum_{j=1}^{\infty} e^{-i\,(j-0.5)\,\omega T} \left[\frac{1}{\left(1 + (j-0.5)2t\,/\,z_0\right)^2} + \left\{ \frac{1}{\left(1 + (j-0.5)2t\,/\,z_0\right)^3} - \frac{1}{\left(1 + (j-0.5)2t\,/\,z_0\right)^2} \right\} \frac{1}{1 + i\,\omega z_0\,/\,c} \right] \tag{1.25}$$

$$T_{12}(\omega) = 2\sum_{j=1}^{\infty} e^{-i\,(j-0.5)\,\omega T} \left[\frac{1}{\left(1 + (j-0.5)2t\,/\,(z_0 + t)\right)^2} + \left\{ \frac{1}{\left(1 + (j-0.5)2t\,/\,(z_0 + t)\right)^3} - \frac{1}{\left(1 + (j-0.5)2t\,/\,(z_0 + t)\right)^2} \right\} \frac{1}{1 + i\,\omega (z_0 + t)\,/\,c} \right] \tag{1.26}$$

$$T_{22}(\omega) = 1 + 2\sum_{j=1}^{\infty} e^{-ij\,\omega T} \left[\frac{1}{\left(1 + j\,2t\,/\,(z_0 + t)\right)^2} + \left\{ \frac{1}{\left(1 + j\,2t\,/\,(z_0 + t)\right)^3} - \frac{1}{\left(1 + j\,2t\,/\,(z_0 + t)\right)^2} \right\} \frac{1}{1 + i\,\omega (z_0 + t)\,/\,c} \right] \tag{1.27}$$

Appendix 2

$$[\Delta K_{hr}] = \frac{\Delta EI}{t^3}\begin{bmatrix} 12 & 6t & -12 & 6t \\ 6t & 4t^2 & -6t & 2t^2 \\ -12 & -6t & 12 & -6t \\ 6t & 2t^2 & -6t & 4t^2 \end{bmatrix} \tag{1.28}$$

$$[\Delta M_h] = \frac{\Delta M}{2}\begin{bmatrix} 1 & 0 & 0 & 0 \\ 0 & 0 & 0 & 0 \\ 0 & 0 & 1 & 0 \\ 0 & 0 & 0 & 0 \end{bmatrix} \tag{1.29}$$

$$[\Delta I_r] = \frac{\Delta I_r}{2}\begin{bmatrix} 0 & 0 & 0 & 0 \\ 0 & 1 & 0 & 0 \\ 0 & 0 & 0 & 0 \\ 0 & 0 & 0 & 1 \end{bmatrix} \tag{1.30}$$

$$[\Delta K_v] = \frac{\Delta EA}{t}\begin{bmatrix} 1 & -1 \\ -1 & 1 \end{bmatrix} \tag{1.31}$$

$$[\Delta M_v] = \frac{\Delta M}{2}\begin{bmatrix} 1 & 0 \\ 0 & 1 \end{bmatrix} \tag{1.32}$$

$$[\Delta K_t] = \frac{\Delta G\,J}{t}\begin{bmatrix} 1 & -1 \\ -1 & 1 \end{bmatrix} \tag{1.33}$$

$$[\Delta I_t] = \frac{\Delta I_t}{2}\begin{bmatrix} 1 & 0 \\ 0 & 1 \end{bmatrix} \tag{1.34}$$

ΔE is the difference in the modulus of elasticity of the pile and soil.

t is the soil segment thickness.

ΔM is the difference in mass of the pile and soil solid cylinders.

ΔI_r is the difference in the mass moment of inertia of the pile and soil solid cylinders within the length t .

A, I, J are the cross section area, the moment of inertia and the torsion constant of the pile respectively.

ΔG is the difference in the shear modulus of the pile and soil.

ΔI_t is the difference in the polar mass moment of inertia of the pile and soil solid cylinders within the length t .

References

Chowdhury I., Dasgupta S.P. (2009) *Dynamics of structure and foundation – a unified approach.* Taylor & Francis Group, London, UK.

Jaya K.P., Prasad A.M. (2002) *Embedded foundation in layered soil under dynamic excitations*. Journal of Soil Dynamics and Earthquake Engineering, Vol. 22, p 485–498.

Jaya K.P., Prasad A.M. (2004) *Dynamic behaviour of pile foundations in layered soil medium using cone frustums*. Géotechnique, Vol. 54, No. 6, p 399–414.

Meek J.W., Wolf J.P. (1994) *Cone models for an embedded foundation.* Journal of the Geotechnical Engineering Division, Proceedings of the ASCE, Vol. 120, No.1, p 60–80.

Meek, J.W. (1995) *Continuum model for built-in piles in layered soil.* Bautechnik, Vol. 72, No. 2, p 116–123 (in German).

Novak M., Aboul-Ella F. (1978) *Impedance functions of piles in layered media.* Journal of the Engineering Mechanics Division, Vol. 104, No. 3, p 643-661.

Novak M., Nogami T., Aboul-Ella F. (1978) *Dynamic soil reactions for plane strain case*. Journal of the Engineering Mechanics Division, Vol. 104, No. 4, p 953-959.

Pradhan P.K., Baidya D.K., Ghosh D.P. (2004) *Dynamic response of foundations resting on layered soil by cone model*. Journal of Soil Dynamics and Earthquake Engineering, Vol. 24, p 425–434.

Schevenels M., Degrande G., François S. (2008) *EDT: An elastodynamics toolbox for MATLAB*. Proceedings of the Inaugural International Conference of the Engineering Mechanics Institute (EM08), Minneapolis, Minnesota, USA.

Schevenels M., François S., Degrande G. (2009) *A MATLAB toolbox for seismic wave propagation.* Proceedings of ISEV2009 - Environmental Vibrations: Prediction, Monitoring, Mitigation and Evaluation, Beijing, China, Vol. 1, p 24-29.

Wolf J.P. (1985) *Dynamic soil-structure interaction.* Prentice Hall, Englewood Cliffs, New Jersey, USA.

Wolf J.P. (1994) *Foundation vibration analysis using simple physical models*. Prentice Hall, Englewood Cliffs, New Jersey, USA.

Wolf J.P. (1998) *Simple physical models for foundation dynamics.* Developments in Geotechnical Engineering, Dynamic Soil-Structure Interaction - Current Research in China and Switzerland, Vol. 83, p 1-70.

Wolf J.P., Deeks A.J. (2004a) *Foundation vibration analysis: a strength-of-materials approach*. Elsevier, Oxford, UK.

Wolf J.P., Meek J.W. (1994b) *Dynamic stiffness of foundation on or embedded in layered soil half-space using cone frustums.* Journal of Earthquake Engineering and Structural Dynamics, Vol. 23, p 1079–1095.

Wolf J.P., Preisig M. (2003) *Dynamic stiffness of foundation embedded in layered half-space based on wave propagation in cones.* Journal of Earthquake Engineering and Structural Dynamics, Vol. 32, p 1075–1098.

Table 1 – Aspect ratios for different types of motion [Wolf, 1994]

	Horizontal motion	Vertical motion	Rocking motion	Torsional motion
Aspect Ratio	$\frac{\pi}{8}(2-\nu)$	$\frac{\pi}{4}(1-\nu)\left(\frac{c_p}{c_s}\right)^2$	$\frac{9\pi}{32}(1-\nu)\left(\frac{c_p}{c_s}\right)^2$	$\frac{9\pi}{32}$

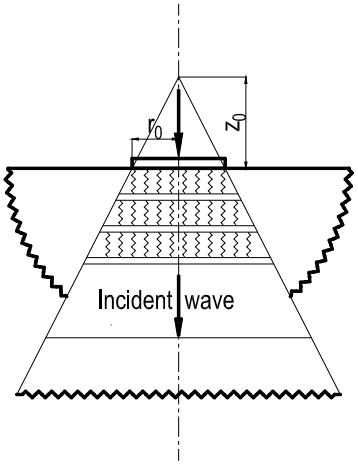

Figure 1 – Cone model of a loaded disk overlying a half-space

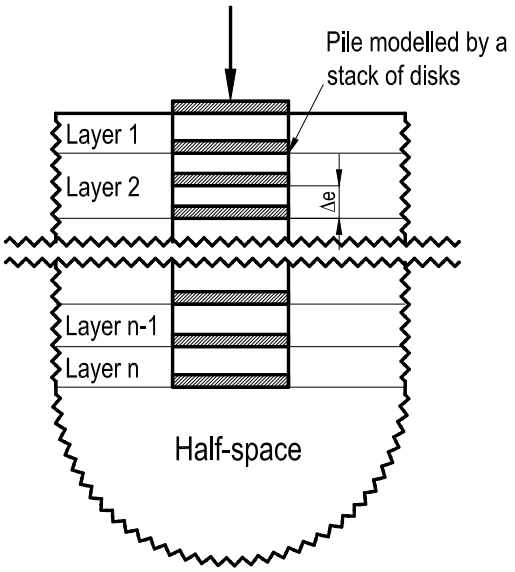

Figure 2 – Stack of disks to model an embedded foundation

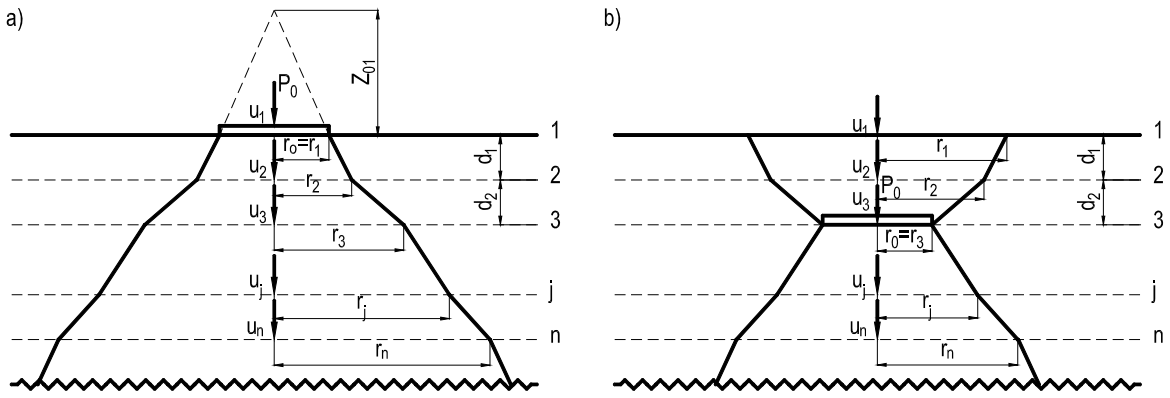

Figure 3 – Backbone cone consisting of cone frustums with varying aspect ratios in a layered half-space. a) Surface disk, b) Embedded disk [Wolf & Meek, 1994b]

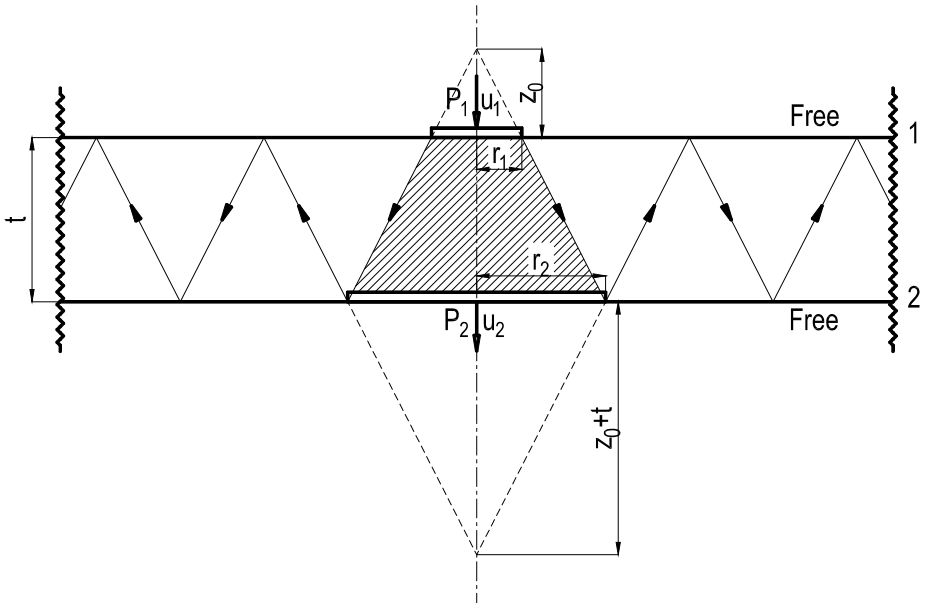

Figure 4 – Cone frustum segment with free surfaces and two disks showing the wave pattern under a vertical load

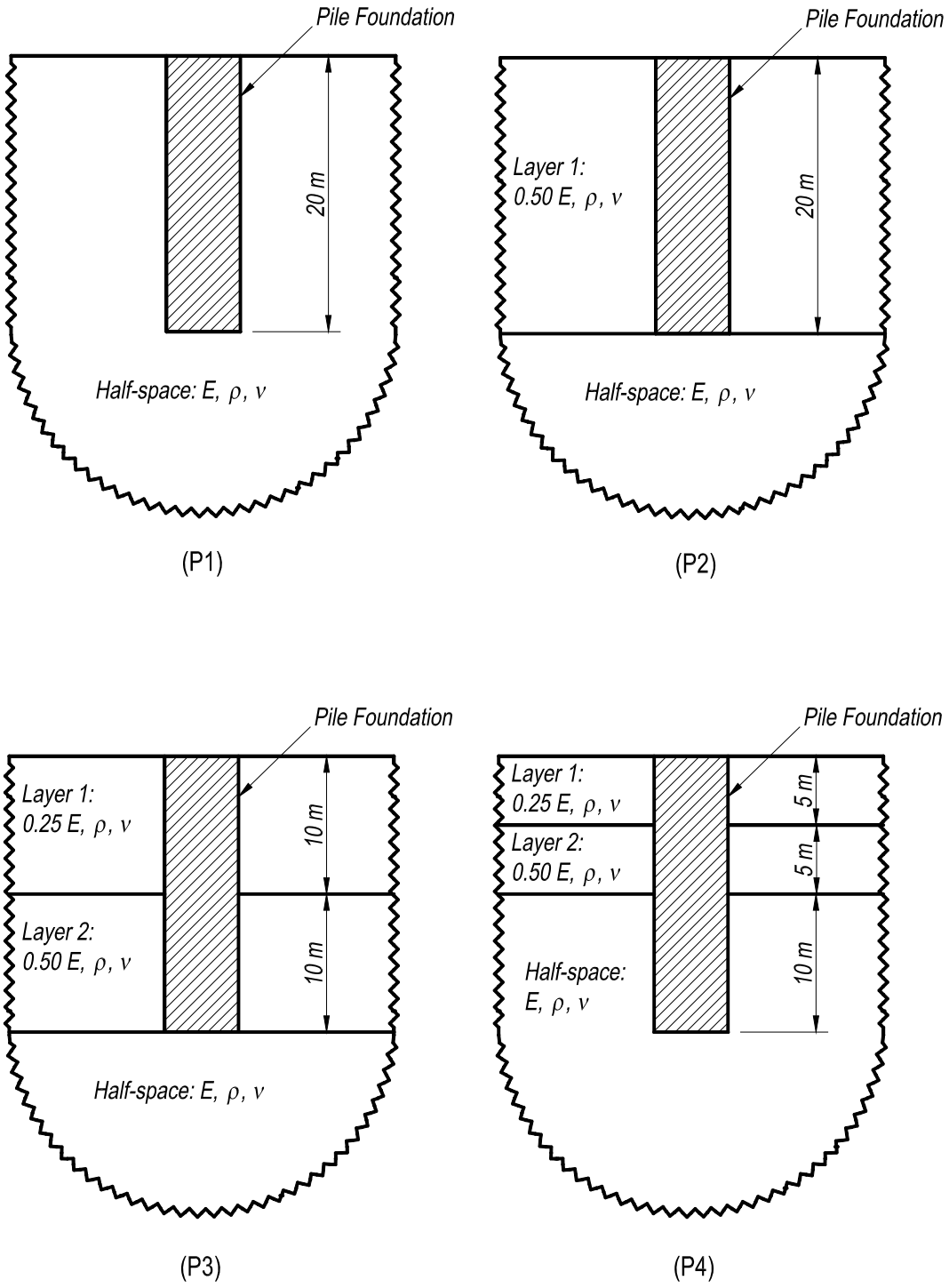

Figure 5 – Pile foundation embedded in four different soil profiles P1, P2, P3 and P4

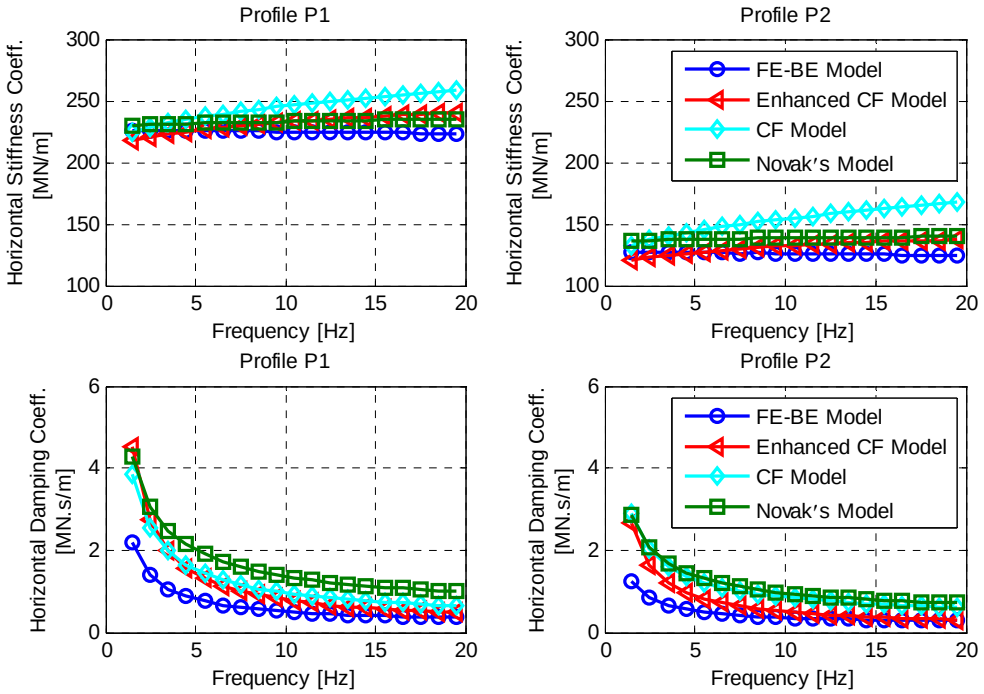

Figure 6 – Horizontal stiffness and damping coefficients of the pile foundation in profiles P1 and P2

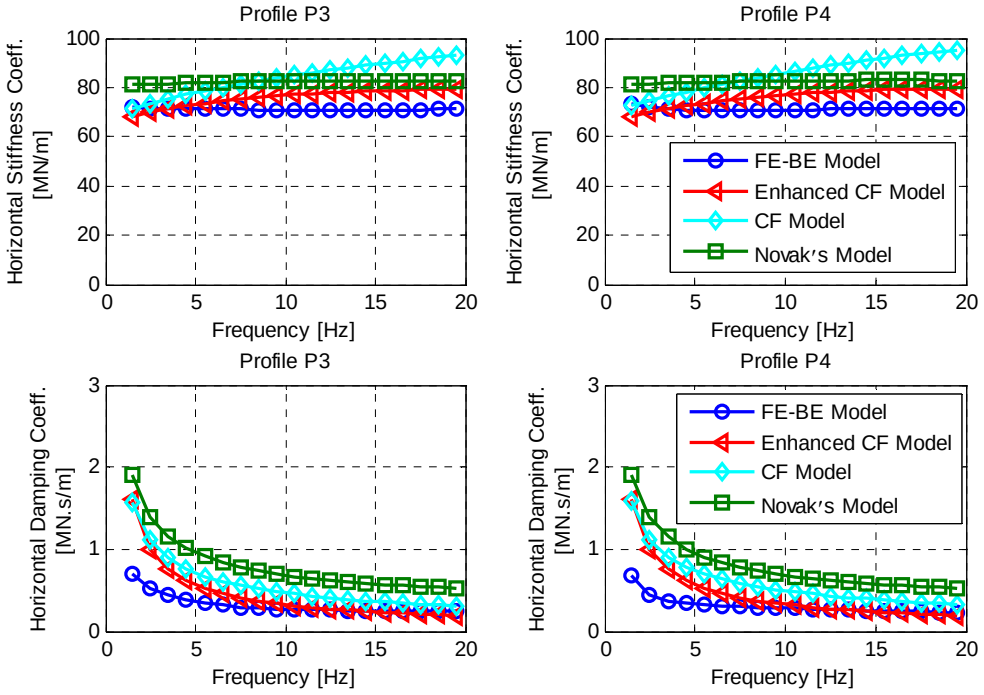

Figure 7 – Horizontal stiffness and damping coefficients of the pile foundation in profiles P3 and P4

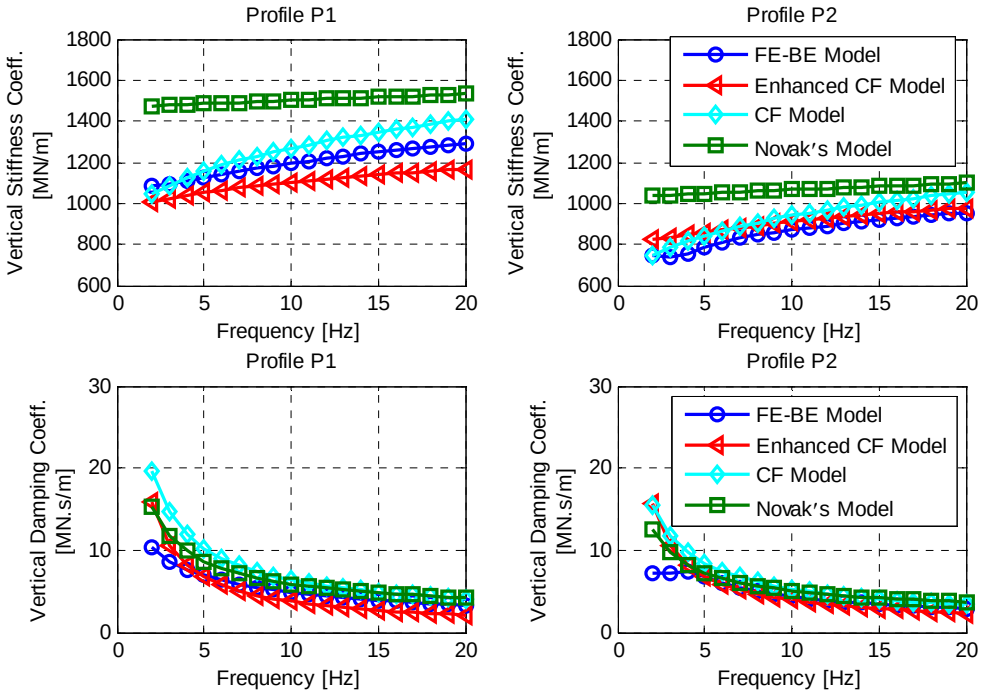

Figure 8 – Vertical stiffness and damping coefficients of the pile foundation in profiles P1 and P2

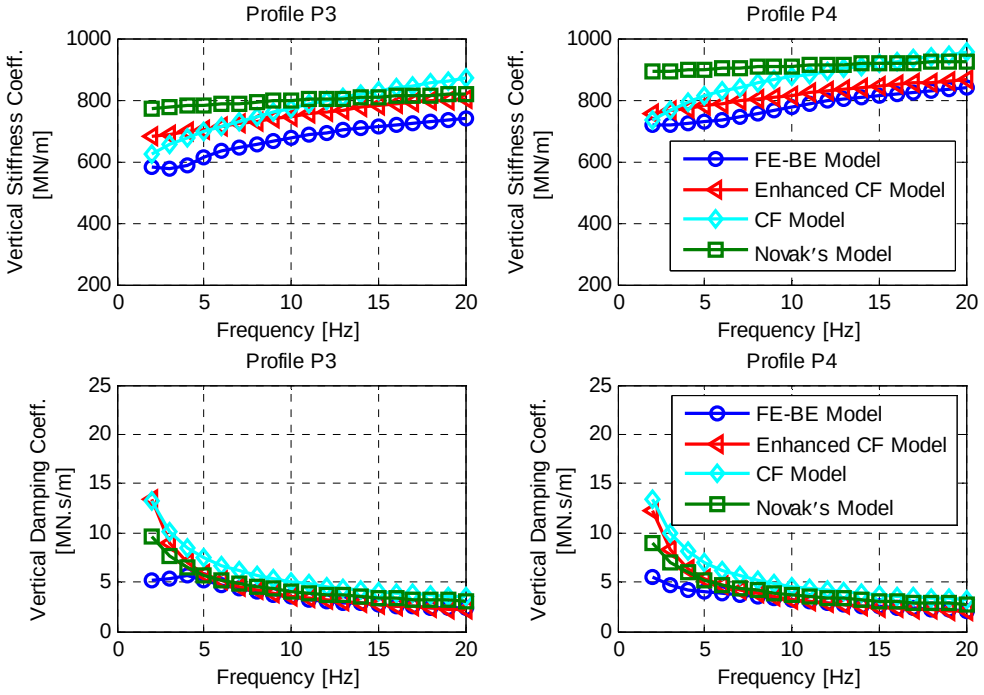

Figure 9 – Vertical stiffness and damping coefficients of the pile foundation in profiles P3 and P4

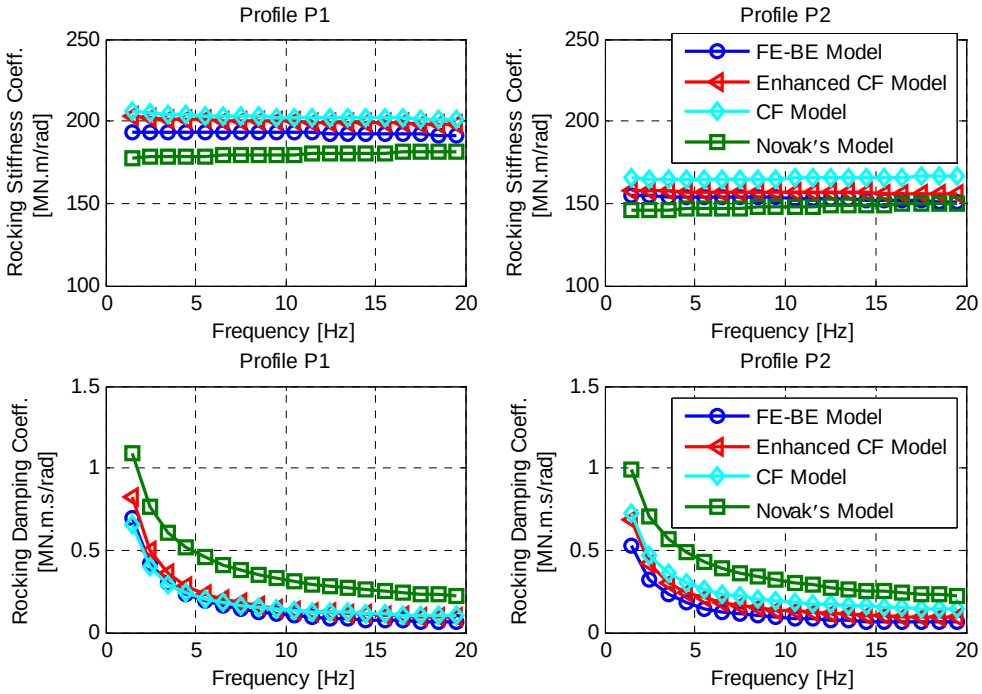

Figure 10 – Rocking stiffness and damping coefficients of the pile foundation in profiles P1 and P2

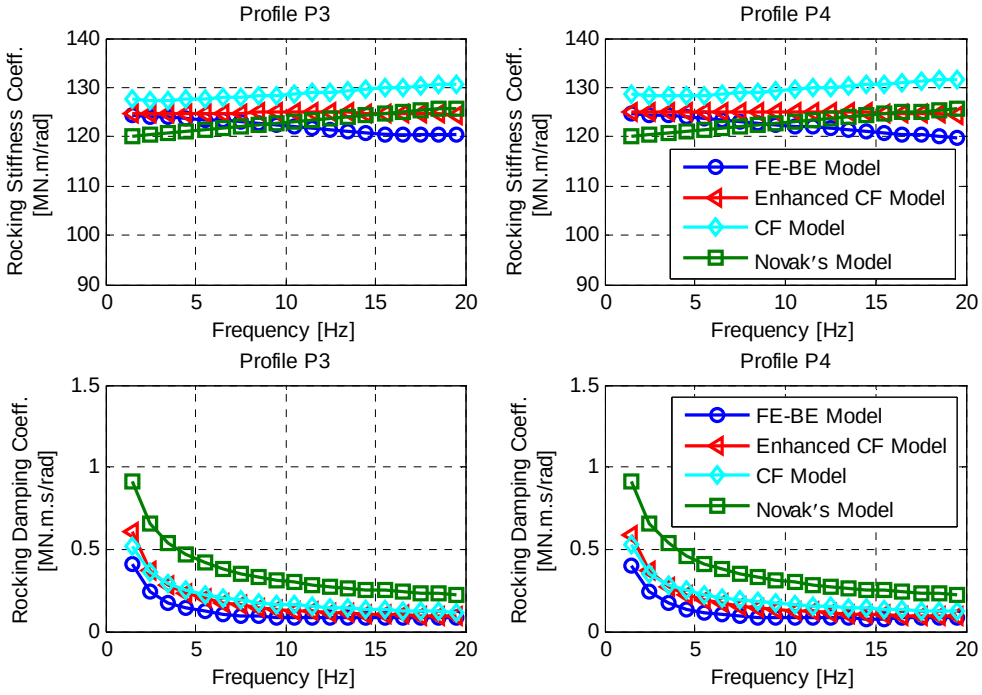

Figure 11 – Rocking stiffness and damping coefficients of the pile foundation in profiles P3 and P4